Available online at www.sciencedirect.com
SCIENCE DIRECT®
Journal of Catalysis 225 (2004) 408–416
JOURNAL OF CATALYSIS
www.elsevier.com/locate/jcat

Comparative study of TiO_2 particles in powder form and as a thin nanostructured film on quartz

Igor N. Martyanov and Kenneth J. Klabunde *

Department of Chemistry, Kansas State University, 111 Willard Hall, Manhattan, KS 66506, USA

Received 11 June 2003; revised 25 March 2004; accepted 7 April 2004

Available online 25 May 2004

Abstract

A sol–gel method was employed to prepare TiO_2 particles in the powder form and on a flat quartz (SiO_2) support. Calcination at progressively higher temperatures caused morphological and structural changes, which were followed by XRD, UV-Vis spectroscopy, AFM, and SEM microscopy. In particular, it was found that annealing at 500 °C leads to the formation of the anatase phase for both TiO_2 on SiO_2 and TiO_2 in the powder form (self-supported). However, after annealing at 800 °C the TiO_2 particles on SiO_2 remained in the anatase form, whereas the anatase phase of self-supported TiO_2 particles was easily converted into the rutile form. TiO_2 particles on SiO_2 remained as individual crystallites even at 800 °C despite the growth of their size, whereas annealing TiO_2 powders at 500 and 800 °C led to bigger crystallites with their eventual sintering to very big particles of micrometer size. Examination of the photocatalytic activity of TiO_2 on SiO_2 and TiO_2 in the powder form in the reaction of acetaldehyde oxidation demonstrated the TiO_2 on SiO_2 superiority with quantum yields significantly higher than that of TiO_2 powder.

Keywords: TiO_2; Powder; Film; SiO_2; Quartz; Temperature; XRD; AFM; UV-Vis; Photocatalysis; Acetaldehyde

1. Introduction

Nanoparticulate TiO_2 remains one of the most promising materials in the field of photocatalysis. Being produced on a large scale, this compound possesses a low toxicity and an excellent chemical stability even in harsh environments. Additionally nanosized TiO_2 was found to be an active photocatalyst in numerous oxidative reactions [1–4]. The atmospheric concentration of oxygen and UV light are all that is needed to drive oxidation of virtually any organic molecules adsorbed at the TiO_2 surface. Since such redox processes can occur at room temperature under solar or artificial UV light, a number of practical applications [5] have been suggested including photoelectrochemical cells [6], antifog windows [7], and various cleaning devices [8].

Recently, acetaldehyde was recognized to be one of the major indoor pollutants. It is thought to appear through oxidation of a wide variety of organic molecules emitted by carpets and other household utilities with outdoor ozone [9]. Being a fairly toxic compound, acetaldehyde can be destroyed with a high quantum yield over UV-illuminated TiO_2 [10].

Nanosized TiO_2 of anatase crystalline form prepared through different pathways is usually used as a photocatalyst. Among all synthetic procedures, preparation of TiO_2 by a sol–gel route remains one of the most attractive. The important advantages of this approach is its great flexibility such as the possibility of preparing powders or films of pure and mixed oxides in nanoparticulate form on a routine basis [11,12].

A typical preparation procedure involves hydrolysis of titanium alkoxides in the presence of acid or base accompanied by polymerization. The reactions written in a very simplified manner can be presented as follows:

$$\equiv\text{Ti–OR} + \text{H}_2\text{O} \rightarrow \equiv\text{Ti–OH} + \text{ROH} \quad (1)$$

hydrolysis,

$$\equiv\text{Ti–OR} + \text{HO–Ti} \rightarrow \equiv\text{Ti–O–Ti}\equiv + \text{ROH} \quad (2)$$

condensation.

* Corresponding author. Fax: (785) 532-6666.
E-mail address: kenjk@ksu.edu (K.J. Klabunde).

0021-9517/$ – see front matter
doi:10.1016/j.jcat.2004.04.019

The resulting gel is later dried under supercritical conditions to yield an aerogel or under ambient conditions to form a xerogel. Deposition of TiO_2 sol on a solid support such as a quartz plate followed by gelation allows the formation of well-adhering TiO_2 films.

The disadvantages of the traditional sol–gel route include the amorphous nature of the as-prepared xerogels, and a high content of the residual organics. Firing of such xerogels at temperatures around 500 °C and higher burns the organic contaminants and crystallizes the sample. However, these processes are often accompanied by a dramatic decrease in the surface areas.

In the present work, we focus our attention on the behavior of TiO_2 deposited on a quartz support as a function of calcination temperature. Unsupported TiO_2 powder was obtained in a similar way and used for comparative purposes. The primary objective of this study was examination of the influence of the SiO_2 support on TiO_2 morphological/structural properties and its impact on TiO_2 photocatalytic activity.

2. Experimental

2.1. Reagents and materials

Titanium(IV) isopropoxide, $Ti(OC_3H_7)_4$ (Aldrich), 2-propanol, and nitric acid (Fisher) were used as received. Distilled water was additionally cleaned prior to its use with a Water Purification System from Millipore Corporation. Quartz UV-type windows and cells were bought from Starna Cells, Inc.

2.2. TiO_2 film/powder preparation

A TiO_2 sol was obtained through rapid addition of the solution containing 5.9 mL $Ti(OC_3H_7)_4$ in 75 mL 2-propanol to the mixture of 0.6 mL H_2O and 0.25 mL HNO_3 in 75 mL 2-propanol. The final molar ratio of starting compounds were: $[H_2O]/[Ti(OC_3H_7)_4] = 2$ and $[HNO_3]/[Ti(OC_3H_7)_4] = 0.2$.

Prior to the film deposition, the quartz support was thoroughly cleaned in hot sulfuric acid overnight, rinsed in distilled water, soaked in a fresh portion of distilled water overnight, rinsed in water again, and dried under ambient conditions.

The film was prepared by dip-coating of the pretreated quartz support into the TiO_2 sol aged for ca. 5 min. The film was first dried at room temperature in air, then at 70 °C, and finally annealed at 200, 500, or 800 °C in air for 4 h.

The TiO_2 powder was made from the same sol used for the TiO_2 film fabrication with the same drying/annealing steps involved.

2.3. TiO_2 film/powder characterization

XRD patterns were recorded with a XDS 2000 Scintac Inc. instrument equipped with Cu-K_α source and operating in 0.02° step mode with 1 s/step acquisition time. The crystallite size of the sample was derived via the Scherer equation with correction for broadening caused by the instrument.

Surface areas of the samples were derived with the multipoint BET method from nitrogen adsorption isotherms measured at 77 K on a NOVA instrument. Prior to the measurements the samples were additionally degassed at 70 °C under dynamic vacuum (10^{-2} Torr) for an hour.

A Cary 500 Scan UV-Vis-NIR spectrophotometer from Varian Analytical Instruments was employed for UV-Vis optical spectra measurements. The spectra of TiO_2 films were recorded in the transmission mode, whereas a diffuse–reflectance accessory with PTFE reference was employed for determination of UV-Vis spectra of the powdered samples.

AFM images of the films were observed with a Multi Mode Atomic Force Microscope from Digital Instrument operating in the tapping mode. A scanning electron microscope from Hitachi Science System was used for obtaining the images of the powdered samples.

2.4. Photocatalytic experiments

Monochromatic illumination (ca. 313 nm) was employed to drive the photocatalytic oxidation of acetaldehyde over TiO_2 samples. The monochromatic illumination was prepared from the light of a 1000 W He(Xe) lamp by passing it through water, neutral density (59670), and interference (56511) filters (all from Oriel Instruments). The light intensity was ca. 7.6 mW/cm^2 (1.2×10^{16} photon/(s cm^2)) as measured with a Power Max 500D laser power meter from Molectron Detector, Inc.

A gas chromatograph equipped with a mass-selective detector (GCMS-QP5000 from Shimadzu) was employed to follow acetaldehyde and carbon dioxide concentrations. The column (phase XTI-5, Restek Corp.) maintained at 40 °C was used to separate the reagents and the products. The quantification of GCMS readings was based on the intensity of $m/z = 44$ peaks (for both acetaldehyde and carbon dioxide) and appropriate calibration curves obtained in separate experiments.

Photocatalytic activity of the TiO_2 films as well as powders was tested in the reaction of acetaldehyde photooxidation at 25 °C. In a typical experiment, a 5-mL quartz cell with a TiO_2 film (ca. 2.5 μg/cm^2 TiO_2) or powder (50 mg/cm^2) placed at a cell wall was filled with air. Later, a mixture of gaseous acetaldehyde and air was passed through the Teflon septum of the cell until concentration of acetaldehyde reached ca. 2000 ppm.

After sealing the cell and acetaldehyde concentration stabilization, the light (ca. 313 nm) was turned on and the

photocatalytic reaction was started. A decrease in the acetaldehyde concentration as well as an increase in the CO_2 concentration was used for quantum yield determination. For this purpose the first six experimental points were fitted with a straight line, the slope of which was later used for the initial rate estimation. The initial quantum yield of the reaction was determined as a ratio of acetaldehyde/carbon dioxide molecules, M, consumed/produced for 1 s to a number of photons, P, adsorbed by TiO_2 (a film or powder) for the same time:

$$\varphi = \frac{M}{P}. \tag{3}$$

Rewritten in terms that can be measured experimentally and expressed in percentage, the quantum yields for acetaldehyde consumption and carbon dioxide formation at the reaction beginning are

$$\varphi_{\text{acetal}} = -\frac{V\,\mathrm{d}[\text{Acetal}]/\mathrm{d}t}{SI_0(1-10^{-D})} \times 100\%, \quad \text{and}$$
$$\varphi_{\text{CO}_2} = \frac{V\,\mathrm{d}[\text{CO}_2]/\mathrm{d}t}{SI_0(1-10^{-D})} \times 100\%, \tag{4}$$

where $\mathrm{d}[\text{Acetal}]/\mathrm{d}t$ and $\mathrm{d}[\text{CO}_2]/\mathrm{d}t$ are the initial rates of acetaldehyde disappearance and carbon dioxide formation (molecule/(s cm^3)), I_0 is the light intensity reaching the sample (1.2×10^{16} photon/s), D is the optical density of the TiO_2 films/powders at 313 nm measured with the spectrophotometer, V is the reactor volume (5 cm^3), and S (cm^2) is the cross section of the light beam. Note that the product of S, I_0, and $(1-10^{-D})$ determines the number of photons absorbed by the photocatalysts per second.

The optical density, D, was determined from adsorption spectra of films and powder according to a standard formula [13].

For films, $D = \log_{10}(\frac{I_\text{i}}{I_\text{t}})$, where I_i is intensity of the incident light inside the spectrophotometer, and I_t is intensity of the transmitted light measured by the spectrophotometer.

For powders, $D = \log_{10}(\frac{I_\text{i}}{I_\text{s}})$, where I_i is intensity of the incident light inside the spectrophotometer, and I_s is intensity of the light diffusively scattered by the sample and measured by the spectrophotometer.

3. Results

XRD patterns of the TiO_2 films on quartz annealed at different temperatures are presented in Fig. 1. As can be seen the films annealed at 70 and 200 °C remained amorphous. Calcination at 500 °C yields TiO_2 in the anatase crystal structure that did not get converted into the rutile form even at 800 °C. The crystallite size derived from XRD data with the Scherer equation was ca. 28 nm for the sample annealed at 500 °C and ca. 52 nm after annealing at 800 °C.

Similar experiments carried out with TiO_2 powders (Fig. 2) revealed an amorphous nature of the TiO_2 particles annealed at 70 and 200 °C, formation of an anatase phase along with a small amount of rutile phase upon firing at 500 °C, and a pure rutile phase for TiO_2 powders treated at 800 °C. Analysis of the broadness of XRD peaks with the Scherer equation suggests that the alteration of the crystalline structure was accompanied by crystallite size growth from 43 nm at 500 °C to more than 100 nm at 800 °C.

UV-Vis data (Fig. 3) are consistent with the changes in crystalline structure observed with the X-ray diffractometer. Indeed, in the case of the TiO_2 films, annealing at 500 °C causes a shift of absorption onset to the red part of the spectrum as it should be when crystallization occurs. However, annealing at 800 °C does not change the position of the absorption onset since no conversion of anatase into rutile phase takes place.

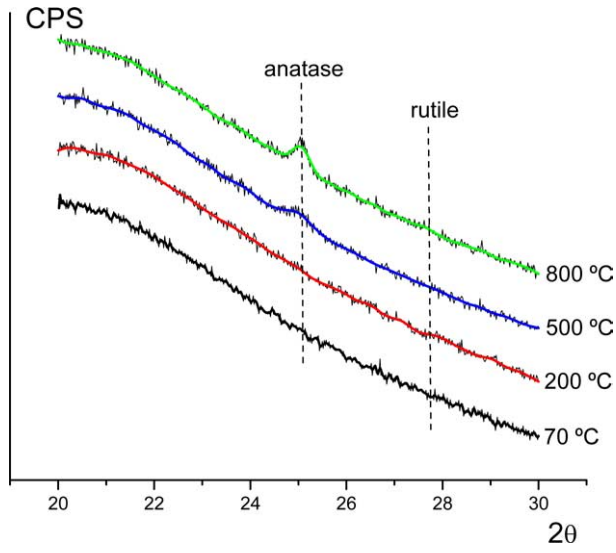

Fig. 1. XRD patterns of the TiO_2 films annealed at different temperatures.

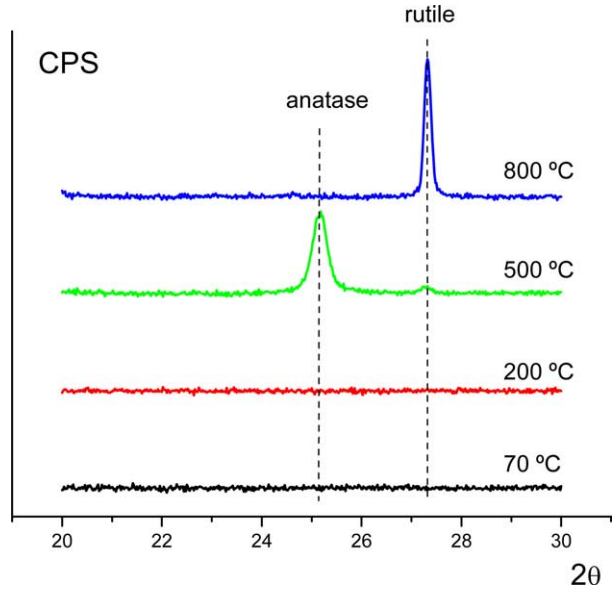

Fig. 2. XRD patterns of the TiO_2 powders annealed at different temperatures.

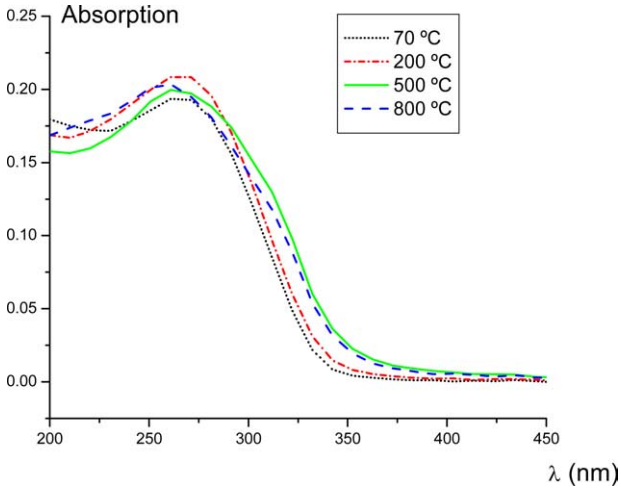

Fig. 3. Transmission UV-Vis spectra of the TiO_2 films on quartz.

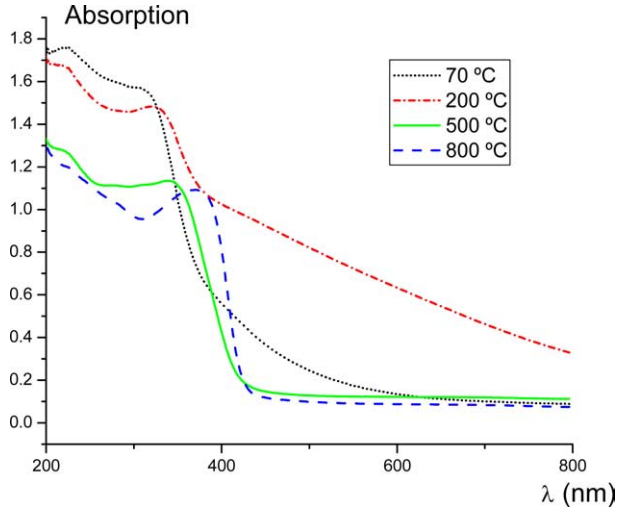

Fig. 4. Diffuse–reflectance UV-Vis spectra of the TiO_2 powders.

Evolution of the UV-Vis spectra of powdered samples was somewhat different. As it can be seen from Fig. 4 annealing the powders at 200 °C causes the strong absorption in the visible region to appear, probably due to incomplete burning/removal of the residual organics. An increase of calcination temperature to 500 °C leads to thermal oxidation of organic contaminants to yield a pure white powder. The further elevation of calcination temperature to 800 °C causes the conversion of anatase into rutile having a smaller band gap with an observable shift of the absorption onset to the red part of the spectral region.

Morphological evolution of TiO_2 film on the SiO_2 support upon calcination at different temperatures is shown in Fig. 5. The general conclusion from AFM images presented is the apparent growth of TiO_2 particles from ca. 10 to 25 nm and then to ca. 50 nm, when annealing temperatures were increased from 200 to 500 °C and then to 800 °C.

Behavior of the TiO_2 particles in the powder form is, however, different. Fig. 6 presents SEM micrographs of the powders annealed at various temperatures. Big aggregates (0.5–5 μm) are observed at any annealing temperature employed. Additional information on TiO_2 powder structure can be inferred from BET surface measurement studies. According to that the surface area of these powders were 340, 390, 1.1, and 0.7 m^2/g for the samples annealed at 70, 200, 500, and 800 °C, respectively. Assuming for simplicity a spherical shape of TiO_2 particles involved, the sizes derived from the surface area studies should be around 3, 2.6, 900, and 1400 nm for 70, 200, 500, and 800 °C annealing temperatures.

The photocatalytic activity of TiO_2 films and powders was tested in the reaction of acetaldehyde oxidation [10]. The initial quantum yields observed are presented in Figs. 7 and 8. An increase in the calcination temperature up to 500 °C increases the film and powder photoactivities. At the same time, whereas heating the TiO_2 film at 800 °C improves its activity even further, a noticeable activity drop was observed for TiO_2 powders. Note also that at any calcination temperature the quantum yield of acetaldehyde consumption and carbon dioxide production over TiO_2 nanocrystals on SiO_2 support were always higher than those over powders. The maximal of quantum yield of CO_2 production for TiO_2/SiO_2 samples achieved after annealing at 800 °C was significantly higher than the maximal activity of TiO_2 powders received after their treatment at 500 °C.

4. Discussion

The initial quantum yield has been chosen as a parameter for comparison of activities of the TiO_2 film and powders. Determined by formula (4), the quantum yield shows how effective TiO_2 particles are in utilization of photons to destroy/produce acetaldehyde/carbon dioxide molecules. For example, the quantum yield of 15% with respect to carbon dioxide production means that 100 photons absorbed by TiO_2 lead to formation of 15 CO_2 molecules. The advantages of quantum yield use for comparison of different system activities are its fundamental nature that can be related to the structure of individual photocatalyst particles and independence of the quantum yield from many parameters that can vary from one experimental setup to another. For example, a twofold increase in the beam cross section, S, would result in twofold increase in the initial reaction rates, $d[Acet]/dt$ and $d[CO_2]/dt$, so that according to formulae (4) no quantum yield change occurs.

When comparing quantum yields measured on films and powders, one may be concerned that for films all TiO_2 particles experience almost similar light intensity, whereas for powders light intensity decreases with penetration depth. Since the quantum yield of a photoreaction can vary with light intensity, the correct approach would require comparison of quantum yields on films and in topmost layers of powders where the intensity of light is close to the incident intensity. A little bit more detailed consideration shows, however, that variation of light intensity with depth can only

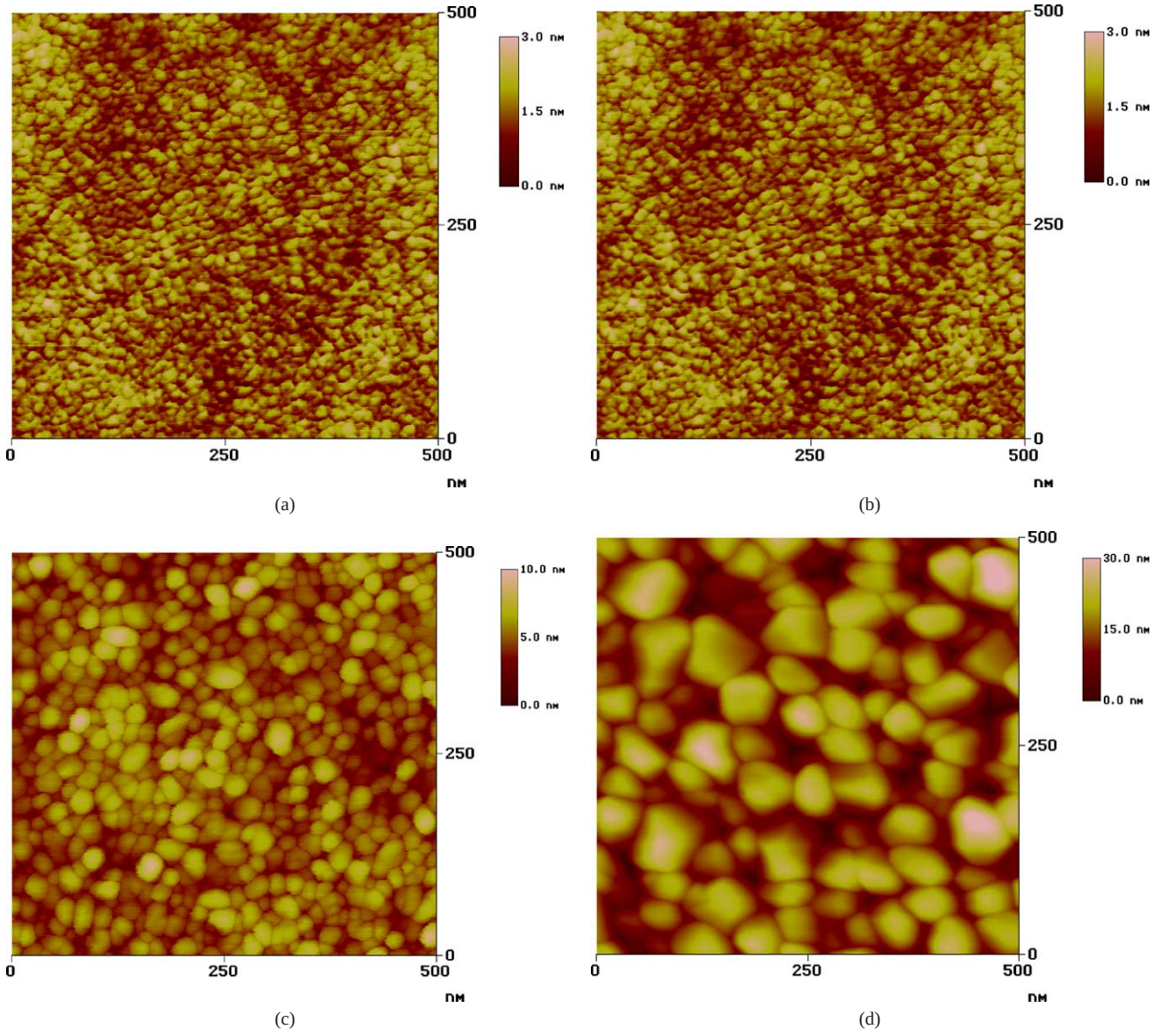

Fig. 5. AFM images of the TiO_2 films (tapping mode) annealed at (a) 70, (b) 200, (c) 500, and (d) 800 °C. According to X-ray diffraction, the particles observed in images (c) and (d) are single crystals of anatase. The films are smooth and clear to the eye.

strengthen our conclusions about the comparative activities of TiO_2 films and powders. Indeed, for powders, the quantum yield measured in this work represents an averaged value over all powder layers. However, since the quantum yield increases with light intensity decrease [10], the quantum yield in the topmost layer is always lower than in layers beneath that and thus lower than the quantum yield averaged over all the powder. In this regard, our experimental observation that the quantum yields for films are higher than for powders means that the quantum yields for films are definitely higher than in the topmost layers of powders experiencing the same light intensity. In other words, the consideration of quantum yield vs light intensity dependence can only reinforce our observation articulated in under Results—TiO_2 particles in a thin layer on quartz are significantly more active than in powders.

Considering the quantum yield data presented in Figs. 7 and 8, it is worth paying additional attention to the carbon balance. The complete oxidation of acetaldehyde can be written as

$$CH_3C(O)H + 2\tfrac{1}{2}O_2 \rightarrow 2CO_2 + 2H_2O. \quad (5)$$

Thus the complete oxidation of one molecule of acetaldehyde must lead to formation of two molecules of carbon dioxide. It is known, however, that oxidation of acetaldehyde proceeds in a pretty complex way and through a number of intermediates before the complete oxidation can be achieved [14,15]. As a result, the formation of intermediates along should decrease the observable rate of CO_2 production with respect to the theoretical value. There is another factor that drives apparent CO_2/acetaldehyde production/consumption ratio in the opposite direction. In-

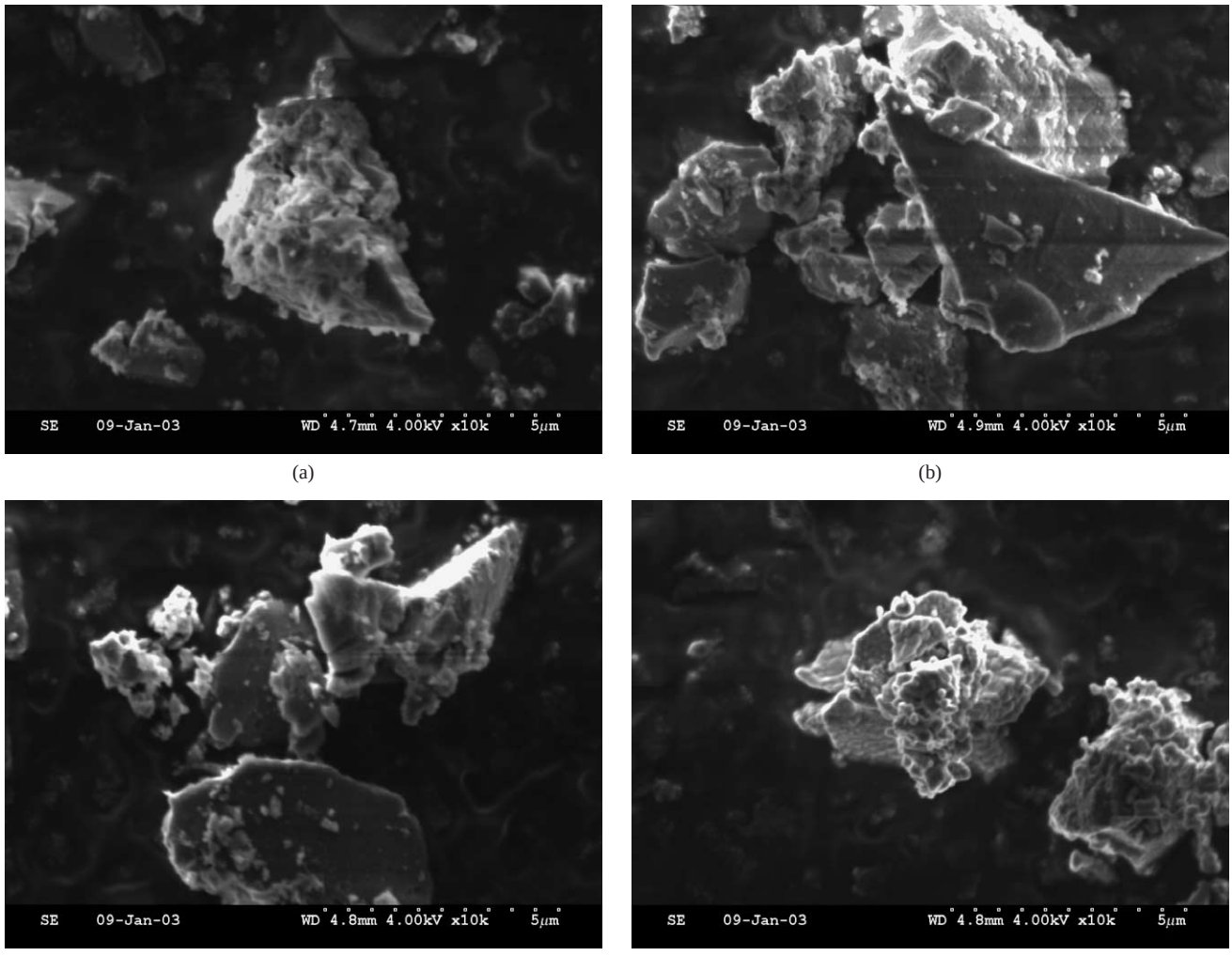

(a) (b)

(c) (d)

Fig. 6. SEM microphotographs of TiO_2 powders annealed at (a) 70, (b) 200, (c) 500, and (d) 800 °C.

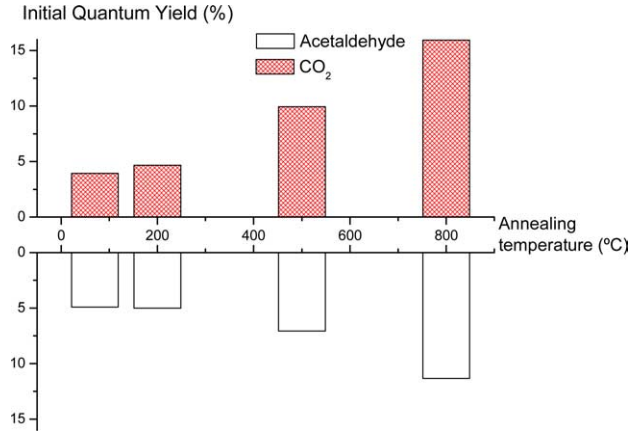

Fig. 7. Influence of calcination temperature on photocatalytic activities of the TiO_2 films. (All quantum yields were measured at the beginning of the reaction.)

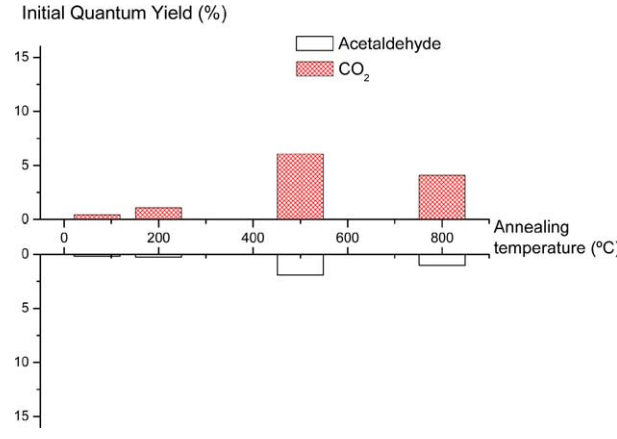

Fig. 8. Influence of calcination temperature on photocatalytic activity of the TiO_2 powders.

deed, adsorption of acetaldehyde was found to be fairly significant when TiO_2 powders were employed as catalysts. Though the gas-phase concentration of acetaldehyde before illumination was the same in all the experiments, the oxidation of absorbed acetaldehyde should lead to formation of additional CO_2. As result CO_2/acetaldehyde quantum yield ratios observed in the experiments with powders and shown

in Fig. 8 exceed two, whereas for films this ratio is slightly higher than unit.

Since capacity of TiO_2 particles with respect to CO_2 adsorption was essentially negligible, the reported quantum yields of gaseous CO_2 production are not expected to be influenced much by CO_2 adsorption. Though the changes in acetaldehyde consumption and carbon dioxide production have a similar trend, the values of initial quantum yield of carbon dioxide production are referred later for TiO_2 film/powder activity comparison.

It is well known that photocatalytic activity of TiO_2 depends on a variety of parameters including but not limited to TiO_2 crystalline structure, crystal/particle size, and the concentration/nature impurities present. A clear discrimination of each parameter influence, however, is not a simple task since an alteration in TiO_2 preparation procedure causes more than one parameter to be affected.

In the present study we have been able to follow a number of parameters to characterize TiO_2 particles with increase in annealing temperature. The behavior of TiO_2 in powder form is rather typical. As annealing temperature increases the TiO_2 particles begin to form crystallites with approximate sizes determined by XRD to be 43 nm at 500 °C and more than 100 nm at 800 °C. The study of the surface area of TiO_2 powders provides information on typical sizes of nonporous particles, each of those can consist of several tightly bound individual crystallites. As noted earlier, the particle sizes determined in this way are around 3, 2.6, 900, and 1400 nm after annealing at 70, 200, 500, and 800 °C correspondingly. Note, for example, that the typical size of the particle of TiO_2 fired at 500 °C, 900 nm, is much higher than the size of an average individual crystallite, 43 nm, at the same annealing temperature.

The SEM images of TiO_2 powders given in Fig. 6 present their overall pictures. The sizes of aggregates, which consist of adhered TiO_2 particles, are in the range of 0.5–5 μm. Compared with the sizes of the particles found with the BET method, one may conclude that aggregates shown in Figs. 6a and 6b are highly porous, whereas the aggregates shown in Figs. 6c and 6d are essentially nonporous.

The morphological evolution of TiO_2 on flat quartz support is different. Indeed, the sizes of individual crystallites determined with XRD give ca. 28 nm at 500 °C and ca. 52 nm at 800 °C. These values are quite consistent with those directly observed by AFM, and the sizes of the individual particles which are ca. 25 and 50 nm at 500 and 800 °C correspondingly. Thus, in contrast to TiO_2 powders, individual TiO_2 crystallites on quartz do not adhere to each other forming nonporous particles but rather stay apart as monocrystallites. Interestingly, TiO_2 particles grow in both powder and on quartz. But the growth of TiO_2 particles in powder proceeds through the growth of individual crystallites as well as through an increase in a number of crystallites sintered. At the same time, the presence of the stable SiO_2 support, which certainly interacts with attached TiO_2 particles, seems to prevent the movement of TiO_2 crystallites as a whole, thus preventing sintering of individual crystallites into bigger particles.

The crystalline phase of TiO_2 remains one of principal factors that determine activities of the photocatalysts. The anatase form of TiO_2 is preferable since anatase rather than rutile is found to be highly active in the photooxidation of organics when oxygen is used as an acceptor of photogenerated electrons [16]. It is interesting, however, that just the opposite is true when the reactions are carried out in the presence of relatively high concentrations of acceptors such as Ag^+ [17] or H_2O_2 [18]. Variation of adsorption capabilities, crystallinity [17], the lower concentration of hydroxide groups on the rutile surface [19], and dissociative nature of water adsorption on rutile [20] were pointed out as the reasons for observed differences in anatase/rutile activities. Formation of close contact between the pure anatase/rutile phases can further improve the activities of the pure anatase/rutile crystalline forms [21]. The space charge formed in the vicinity of the anatase–rutile interphase is thought to be responsible for photogenerated electron/hole separation and high activity of commercially available TiO_2 Degussa P25 [22].

For the purpose of oxidation of organic compounds with molecular oxygen, it is important to have TiO_2 in anatase form as well as to keep TiO_2 in a nanosized range where the highest activity was observed [23–26]. Unfortunately, the TiO_2 crystalline structure and average particle size are often related to each other and both change as annealing temperature increases. It is a general tendency that an annealing temperature increase causes TiO_2 particles to grow (loss of TiO_2 surface area), while the crystalline structure changes from amorphous into anatase and then into the most stable rutile [20]. As observed in this work, a tremendous particle growth from 2.6 to 900 nm in the 200 to 500 °C range that accompanied crystallization of amorphous TiO_2 is consistent with literature data [27]. Interestingly, the particle growth can be partially suppressed when residual organic is partially removed from the sample before calcination [27] or when highly crystalline TiO_2 particles are prepared in the solution [28].

As seen for powders, there are at least two factors, particle size and crystalline structure, which can be expected to drive the photocatalytic activity of TiO_2 in different directions as annealing temperature increases. Indeed, as annealing temperature increases from 200 to 500 °C, the powdered TiO_2 converts in highly active anatase form. However, this is accompanied by the tremendous particle size growth from 2.6 to 900 nm. Since the increase of photoactivity is actually observed (Fig. 8), the change in the crystalline structure seems to be the determining factor in this annealing temperature range. The further annealing temperature increase to 800 °C results in the further growth of TiO_2 particles as well as conversion of anatase into generally less active rutile. From 500 to 800 °C, both factors are expected to drive the TiO_2 particle activities down and this is observed in experiment (Fig. 8).

The preparation of TiO_2 particles on the quartz support changes the morphological behavior of TiO_2 with annealing temperature increase. Besides the different particle size evolution considered above, the presence of SiO_2 under TiO_2 was found to be important for stabilization of the anatase form of titanium dioxide. Considering the behavior of TiO_2 on the quartz support it is important to relate it to the literature data on TiO_2/SiO_2 powders and TiO_2/SiO_2 films. In particular, the insertion of Si^{4+} into TiO_2 particles was found to be beneficial for stabilizing the anatase form of TiO_2 [29,30]. It was suggested that along with Si–O–Ti bond formation the main reason of this influence is expulsion of Si^{4+} from TiO_2 at high temperatures. The SiO_2 shell formed in this process surrounds TiO_2 particles, preventing their further growth so that nucleation of rutile becomes a less likely event [29]. As to TiO_2 on quartz studied here, formation of SiO_2 around TiO_2 particles is unlikely since the quartz support was found to be stable at any temperature employed. Another mechanism has to be operational to stabilize TiO_2 in the anatase form.

The thin films of TiO_2 on SiO_2 have been studied earlier [31–35]. Similar to our results stabilization of the anatase form of TiO_2 on SiO_2 at high annealing temperatures was observed [35]. In that instance, however, the TiO_2 film was prepared from a preformed TiO_2 colloidal solution. The TiO_2 particles did not grow with temperature. Thus two possible reasons for anatase stability were assumed:

The small size of the TiO_2 particles (it was argued that the TiO_2 particle should be at least 20 nm in size to make the anatase to rutile phase transformation possible); and second, a TiO_2/SiO_2 interaction.

The different preparation procedure of TiO_2 on SiO_2 in the present study results in somewhat different TiO_2 behavior. The particles do grow with temperature while remaining in the anatase form. This observation points at the interaction of TiO_2 with the SiO_2 support as being the crucial factor for stabilization of the anatase phase of the otherwise growing TiO_2 particles.

The influence of SiO_2 on photocatalytic activities of TiO_2/SiO_2 powders was studied earlier. The reactions were conducted in the aqueous phase and the positive as well as negative influences of silica additives on TiO_2 photocatalytic activities have been established when, correspondingly, cationic and anionic organic molecules were used as probes [30,36]. The key point here was suggested to be the charge of TiO_2/SiO_2 particles that becomes more negative as SiO_2 content increases, facilitating adsorption of organic counterions [37].

Since in the present study the reaction occurs at the gas/solid interface, the above noted mechanism of SiO_2 influence is hardly operational. The substantial increase in the reaction quantum yield and, hence, in utilization of absorbed photons, when TiO_2 is on quartz, would be attributed to structural peculiarities of the TiO_2 particles. In this respect, the TiO_2 particles on SiO_2 are superior to TiO_2 particles in powder, since TiO_2 particles on SiO_2 are smaller in size, consist of a single crystallite (thus less defective than TiO_2 particles in powders), and exist in a highly photocatalytically active anatase crystalline form at 500 and 800 °C.

5. Conclusions

Comparison of TiO_2 films with analogously prepared TiO_2 powders highlights a significant influence of the SiO_2 support on structure, on morphology, and eventually on photocatalytic activities of TiO_2 particles. In contrast to the unsupported TiO_2 powders, TiO_2 nanocrystals on SiO_2 remain in a highly photocatalytically active anatase form even at 800 °C. At all temperatures studied TiO_2 particles on SiO_2 remain well spread out with their sizes being always smaller than in the powders. The annealing temperature increase causes the TiO_2 crystallites/particles on SiO_2 and in powder form to grow. The way it happens in each case is, however, different. Indeed, during high-temperature treatment of the TiO_2 powders, the growth of individual crystallites is accompanied by their sintering into even bigger particles. In contrast to that, TiO_2 crystallites on SiO_2 remain significantly restricted in motion. As a result no significant sintering occurs, thus, minimizing capture/recombination of photogenerated electrons/holes at intercrystalline boundaries, and facilitating formation of low defective TiO_2 particles with high photocatalytic activities.

Acknowledgment

Financial support of this work from ARO through a MURI grant (DAAD 19-01-10619) is acknowledged with gratitude.

References

[1] A.L. Linsebigler, G. Lu, J.T. Yates Jr., Chem. Rev. 95 (1995) 735.
[2] M.A. Fox, M.T. Dulay, Chem. Rev. 93 (1993) 341.
[3] M.R. Hoffmann, S.T. Martin, W. Choi, D. Bahnemann, Chem. Rev. 95 (1995) 69.
[4] A. Fujishima, T.N. Rao, D.A. Tryk, J. Photochem. Photobiol. C: Photochem. Rev. 1 (2000) 1.
[5] M. Anpo, Pure Appl. Chem. 72 (7) (2000) 1265.
[6] M. Gratzel, Nature 414 (2001) 338.
[7] R. Wang, K. Hashimoto, A. Fujishima, M. Chikuni, E. Kojima, A. Kitamura, M. Shimohigoshi, T. Watanabe, Nature 338 (1997) 431.
[8] O. Lergini, E. Oliveros, A.M. Braun, Chem. Rev. 93 (1993) 671.
[9] R. Reiss, P.B. Ryan, S.J. Tibbettes, P. Koutrakis, J. Air Waste Manag. Assoc. 45 (1995) 811.
[10] Y. Ohko, D.A. Tryk, K. Hashimoto, A. Fujishima, J. Phys. Chem. B 102 (1998) 2699.
[11] L.L. Hench, J.K. West, Chem. Rev. 90 (1990) 33.
[12] J.A. Schwarz, C. Contescu, A. Contescu, Chem. Rev. 95 (1995) 477.
[13] R.C. Weast (Ed.), Handbook of Chemistry and Physics, fifty fourth ed., CRC Press, Boca Raton, FL, 1973, p. E-247.
[14] D.S. Muggli, K.H. Lowery, J.L. Falconer, J. Catal. 180 (1998) 111.
[15] D.S. Muggli, J.T. McCue, J.L. Falconer, J. Catal. 173 (1998) 470.

[16] H. Kominami, S. Murakami, J. Kato, Y. Kera, B. Ohtani, J. Phys. Chem. B 106 (2002) 10501.
[17] S. Nishimoto, B. Ohtani, H. Kajiwara, T. Kagiya, J. Chem. Soc., Faraday Trans. 1 81 (1985) 61.
[18] A.P. Rivera, K. Tanaka, T. Hisanaga, Appl. Catal. B 3 (1993) 37.
[19] Z. Ding, G.Q. Lu, P.F. Greenfield, J. Chem. Phys. B 104 (2000) 4815.
[20] K.I. Hadjiivanov, D.G. Klissurski, Chem. Soc. Rev. 25 (1) (1996) 61.
[21] T. Kawahara, Y. Konishi, H. Tada, N. Tohge, J. Nishii, S. Ito, Angew. Chem. Int. Ed. 41 (2002) 2811.
[22] R.I. Bickley, T. Gonzalez-Carreno, J.S. Less, L. Plamisano, R.J.D. Tilley, J. Solid State Chem. 92 (1991) 178.
[23] M. Anpo, T. Shima, S. Kodama, Y. Kubokawa, J. Phys. Chem. 91 (1987) 4305.
[24] M. Tomkiewicz, Catal. Today 58 (2000) 115.
[25] Z. Zhang, C.-C. Wang, R. Zakaria, J.Y. Ying, J. Phys. Chem. B 102 (1998) 10871.
[26] A.J. Maira, K.L. Yeung, C.Y. Lee, P.L. Yue, C.K. Chan, J. Catal. 192 (2000) 185.
[27] L.K. Campbell, B.K. Na, E.I. Ko, Chem. Mater. 4 (1992) 1329.
[28] H. Kominami, M. Kohno, Y. Takada, M. Inoue, T. Inui, Y. Kera, Ind. Eng. Chem. Res. 38 (1999) 3925.
[29] K. Okada, N. Yamamoto, Y. Kameshima, A. Yasumori, J. Am. Ceram. Soc. 84 (7) (2001) 1591.
[30] C. Anderson, A.J. Bard, J. Phys. Chem. B 101 (1997) 2611.
[31] B.E. Yoldas, Appl. Opt. 21 (16) (1982) 2960.
[32] L. Hu, T. Yoko, H. Kozuka, S. Sakka, Thin Solid Films 219 (1992) 18.
[33] A.M. Peiro, J. Peral, C. Domingo, X. Domenech, J.A. Ayllon, Chem. Mater. 13 (2001) 2567.
[34] M.C. Blount, D.H. Kim, J.L. Falconer, Environ. Sci. Technol. 35 (2001) 2988.
[35] T.L. Hanley, V. Luca, I. Pickering, R.F. Howe, J. Phys. Chem. B 106 (2002) 1153.
[36] C. Anderson, A.J. Bard, J. Phys. Chem. 99 (1995) 9882.
[37] H. Tada, Y. Kubo, M. Akazawa, S. Ito, Langmuir 14 (1998) 2936.